

Effect Of Cobalt Doping On The Optical Properties Of Magnesium Cobalt Oxide Nanofilm Grown By Electrodeposition Method

N.S. Umeokwonna, A.J. Ekpunobi, P.I Ekwo

Department of Industrial Physics Chukwuemeka Odumegwu Ojukwu University Uli, Anambra state, Nigeria.
Department of Physics and Industrial Physics Nnamdi Azikiwe University, Awka, Anambra State, Nigeria
Email: nicksunny87@yahoo.com

ABSTRACT: Cobalt doped Magnesium Oxide nanofilms were grown by electrodeposition method using heptahydrated Magnesium tetraoxosulphate (VI) salt as source of Magnesium ion, Citric acid as oxidizing agent. Hexahydrated Cobalt Chloride salt was used as source of Cobalt ion and Sodium hydroxide as pH adjuster. The percentage doping was varied from 3% to 23% in intervals of 5%. Results of the study show that the optical properties viz; absorbance, reflectance, refractive index, extinction coefficient, electrical conductivity, complex dielectric constant and optical conductivity are directly proportional to percentage doping with cobalt while transmittance is inversely proportional. The film exhibits low absorbance, reflectance, and high transmittance in all the regions of electromagnetic spectrum.

Keywords: Optical properties; Doping; nanofilm; electrodeposition

1. INTRODUCTION

This research is aimed at growing Magnesium cobalt oxide nanofilms by electrodeposition method and determining the effect of cobalt doping on the optical properties with a view to ascertaining the possible applications. MgO structure is similar to the well-known NaCl structure [1]. Many techniques have been used to deposit MgO thin film such as spray pyrolysis [2], pulsed laser deposition [3], RF sputtering [4], sol-gel spin casting [5], ion beam-assisted deposition [6], metallorganic chemical vapor deposition (MOCVD) [7]. MgO has the advantages of a wide band gap, low optical loss, and refractive index (≈ 1.7) that permits confined optical modes in ferroelectric materials [8]. MgO thin films have been widely used as a chemically stable buffer layer for the deposition of high T_c superconducting films and perovskite-type ferroelectric films because of its good lattice matching with mentioned materials and low chemical reactivity [9]. Magnesium oxide is one of several materials used as thin insulating layers in electronic devices [10]. MgO thin films have been proposed for use as a protective coating on the phosphor screens [11], a passivation layer in high-electron-mobility transistors [12] and a substrate for carbon nanotubes growth [13]. Many ferroelectric and superconducting oxide films, such as PZT, LiNbO₃, BaTiO₃ and YBa₂Cu₃O₇, etc, have been prepared on Si substrates using MgO as an intermediate layer [14]. Nanosized MgO could be used for improving the transesterification reaction at the supercritical/subcritical temperatures [15], decontamination of chemical warfare agents, reducing chlorofluorocarbons [16] and for reactive

adsorbents [17]. MgO thin films have also been applied as protecting layers of dielectrics to improve the discharge characteristics and the panel's lifetime in an ac-plasma display panel (ac-PDP) [18]. Nano-MgO is desirable for a potent disinfectant against bacteria, spores and viruses after adsorption of halogen gases due to the existence of superoxide (O_2^-) anions at the corners, edges, or surfaces of cubic MgO particles [19].

2. MATERIALS AND METHODS

ITO used as deposition substrates were washed with detergent and rinsed three times with distilled water. They were soaked in acetone for fifteen minutes to degrease them. The substrates were rinsed again in distilled water three times without any body contact to avoid contamination, then immersed in a beaker almost half-full of distilled water and put inside Shanghai ultrasonics (SY-180) for ultrasonic bath for ten minutes. They were again brought out using clean forceps, put in another clean dry beaker, and put inside the oven for ten minutes for drying. The slides ready for use were handled with clean forceps to avoid contamination. The precursors for deposition of nanofilms of MgCo₂O₄ with various percentages of Cobalt dopant are Heptahydrated Magnesium tetraoxosulphate (vi) salt as source of Magnesium ion, Citric acid as oxidizing agent, Hexahydrated Cobalt Chloride salt as source of cobalt ion and sodium hydroxide as pH adjuster. The deposition was carried out at room temperature of 303K, pH of 8.6, deposition time of ten minutes, and deposition voltage of 10V. Constant concentrations and volumes of Citric acid and Sodium hydroxide were used while the concentrations of MgSO₄·7H₂O and CoCl₂·6H₂O were varied in accordance with the percentage doping as shown in the table 1. The deposited films were annealed at 200°C for thirty minutes. Characterization of absorbance and percentage transmittance of the films was done with UV/Visible spectrophotometer while other optical properties were calculated accordingly. Characterization of structural property was done by X-Ray diffraction (XRD) while compositional characterization was done with X-Ray

-
- N. S Umeokwonna¹, A. J. Ekpunobi², P. I. Ekwo²
 - Department of Industrial Physics, Chukwuemeka Odumegwu Ojukwu University, Uli, Anambra State, Nigeria
 - Department of Physics and Industrial Physics, Nnamdi Azikiwe University, Awka, Anambra State, Nigeria

fluorescence(XRF) spectrometer. Optical micrograph of the film was done with Olympus microscope.

Table 1: Variation of percentage doping for MgCo₂O₄ nanofilm

Reaction bath	MgSO ₄ .7H ₂ O		Citric acid		CoCl ₂ .6H ₂ O		NaOH		Deposition voltage(V)	pH	% Doping	Time (mins)
	Conc.(M)	Vol.(ml)	Conc.(M)	Vol.(ml)	Conc.(M)	Vol.(ml)	Conc.(M)	Vol.(ml)				
N ₂₃	0.049	15	0.05	30	0.001	15	1	6	10	8.6	3	10
N ₁₄	0.046	15	0.05	30	0.004	15	1	6	10	8.6	8	10
N ₂₄	0.043	15	0.05	30	0.006	15	1	6	10	8.6	13	10
N ₂₅	0.041	15	0.05	30	0.009	15	1	6	10	8.6	18	10
N ₂₆	0.039	15	0.05	30	0.011	15	1	6	10	8.6	23	10

3.0: THEORY/CALCULATIONS

3.1: Analysis of optical properties

The following mathematical tools were applied in the analysis of the following optical properties

3.1.1: Reflectance

The Reflectance of the films was calculated using the relation according to Rubby *et al* (2011) [20]:

$$R = 1 - (A + T)$$

Where A = absorbance, T = transmittance . However the absorbance and transmittance were obtained by the spectrophotometer characterization.

3.1.2: Refractive index (n)

Employing the mathematical relation as given by Rubby *et al* (2011) [20], the refractive index of the films was calculated using the relation:

$$n = \frac{1 + \sqrt{R}}{1 - \sqrt{R}}$$

Where R = reflectance

3.1.3: Absorption coefficient (α)

The absorption coefficient of the films was calculated using the relation as given by:

$$\alpha = \frac{A}{\lambda}$$

Where A = Absorbance and λ = wavelength

3.1.4: Extinction coefficient (k)

Extinction coefficient of the films was determined using the relation as expressed by Nabeel (2011) [21], thus:

$$k = \frac{\alpha \lambda}{4\pi}$$

Where α = absorption coefficient and λ = wavelength

3.1.5: Optical conductivity (σ_o)

By the mathematical relation according to Sharma *et al* (2007) [22], the optical conductivity of the films was calculated thus:

$$\sigma_o = \frac{\alpha n c}{4\pi}$$

Where α = absorption coefficient, n = refractive index and c = velocity of light

3.1.6: Electrical conductivity (σ_e)

Electrical conductivity of the films was calculated using the relation;

$$\delta_e = \frac{2\pi\sigma_o}{\alpha}$$

Where σ_o = optical conductivity and α = absorption coefficient.

3.1.7: Complex dielectric constant (ε_c)

This parameter was calculated by the relation according to Chopra (1969)[23], thus:

$$\epsilon_c = \epsilon_r + \epsilon_i$$

Where ε_r = n² - k² = real dielectric constant and ε_i = 2nk = imaginary dielectric constant., Nabeel (2011) [21],

3.2: Structural analysis

3.2.1: Average crystallite size (D)

The average crystallite size of the films was calculated using the Debye-Scherrer formular thus:

$$D = \frac{k\lambda}{\beta \cos\theta}$$

Where shape factor k ≈ 0.9 , λ = wavelength of the X-ray radiation,

β = fullwidth at half maximum(FWHM)of the diffraction path, θ = diffraction angle

3.2.2: Dislocation density (δ)

This can be evaluated from Williamson and Smallman's formular thus:

$$\delta = \frac{1}{D^2} \text{ (lines/m}^2\text{)}$$

3.2.3: Microstrain (ε)

This is calculated using the relation,

$$\epsilon = \frac{\beta \cos\theta}{4}$$

4.0 : RESULTS

4.1.: Absorbance

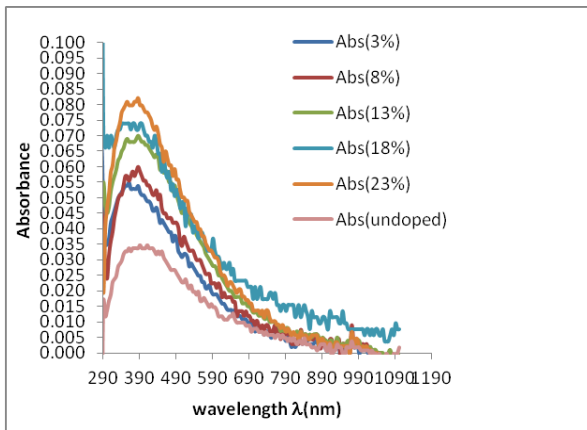


Fig. 1: Variation of absorbance with percentage doping for $MgCo_2O_4$ nanofilm.

From fig. 1, Magnesium Cobalt oxide and magnesium oxide nanofilms generally exhibit low absorbance, maximum value (0.08=8%) for 23% doped, the undoped has maximum value of 0.035=3.5%. However, absorbance of the films is maximum in the ultra violet region and decreases to zero in the near infra red region of the electromagnetic spectrum.. From the result, it is observed that the absorbance increases with increasing percentage doping.

4.2: Transmittance

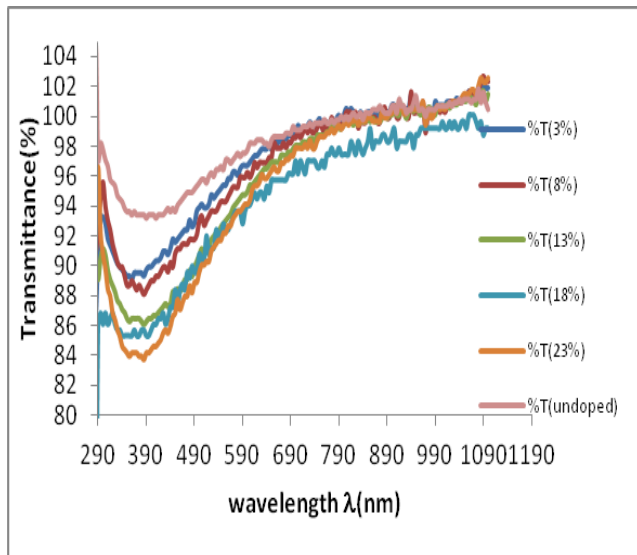


Fig. 2: Variation of transmittance with percentage doping for $MgCo_2O_4$ nanofilm.

From fig. 2, the transmittance of the films is generally high, with minimum value (84%) in the UV region and increases to 100% in the NIR of electromagnetic spectrum. The transmittance decreases with increasing percentage doping with cobalt.

4.3: Reflectance

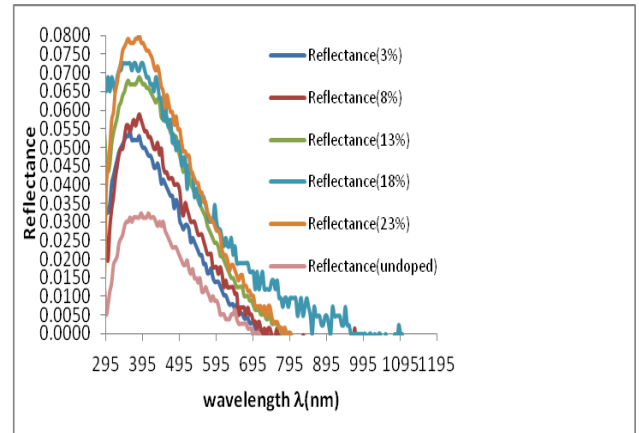


Fig. 3: Variation of reflectance with percentage doping for $MgCo_2O_4$ nanofilm.

From fig. 3, the reflectance of the film is generally low, with maximum value in the UV region (0.0781 ≈ 7.8%) and decreases to zero in the NIR region of electromagnetic spectrum. The reflectance increases with increasing percentage doping with cobalt.

4.4: Refractive index

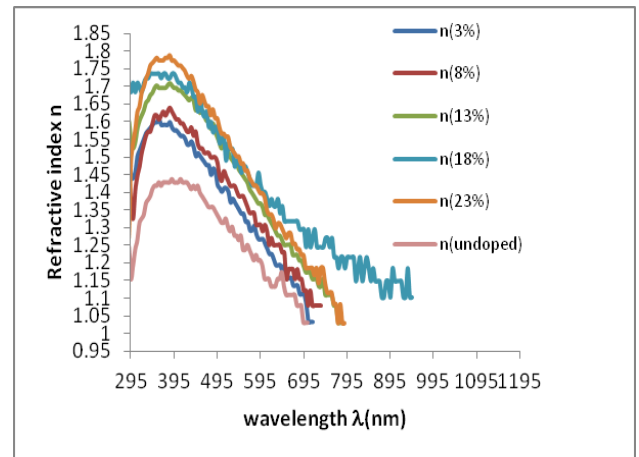


Fig. 4: Variation of refractive index with percentage doping for $MgCo_2O_4$ nanofilm.

From fig. 4, the doped films exhibit high refractive index (< 1.59) in the UV region and decrease to minimum in the VIS-NIR regions of electromagnetic spectrum. Undoped film has maximum refractive index of 1.4 in UV region. The refractive index increases with increasing percentage doping with cobalt.

4.5: Extinction coefficient

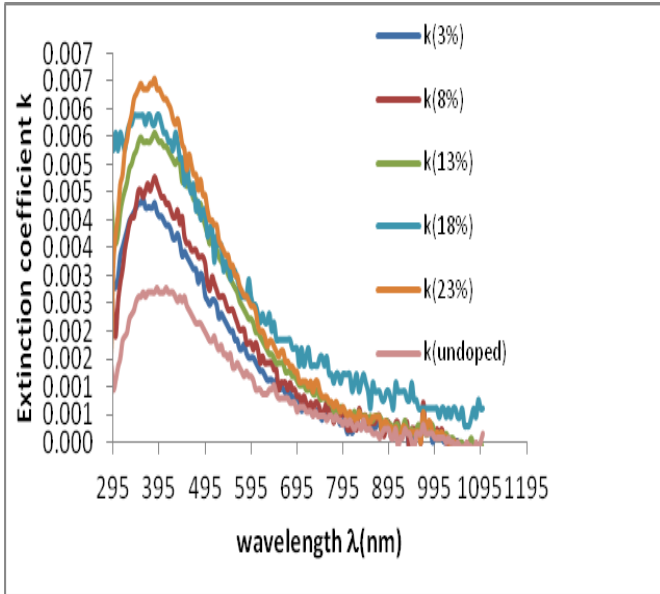


Fig. 5: Variation of extinction coefficient with percentage doping for MgCo₂O₄ nanofilm.

From fig. 5, extinction coefficient of the film is maximum in the UV region and decreases to zero in the NIR region of electromagnetic spectrum. The extinction coefficient increases with increasing percentage doping with cobalt.

4.6: Electrical conductivity

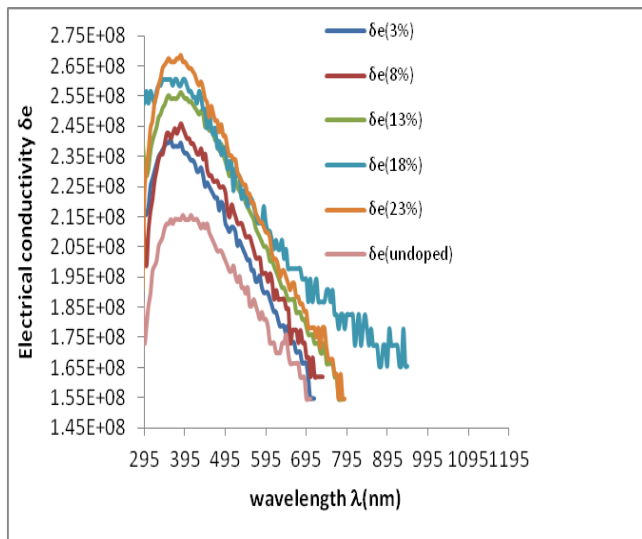


Fig. 6: Variation of electrical conductivity with percentage doping for MgCo₂O₄ nanofilm.

Result as shown in fig. 6, shows that electrical conductivity of the film is maximum in the UV region and decreases to minimum in the visible-NIR region of electromagnetic spectrum. The electrical conductivity increases with increasing percentage doping with cobalt.

4.7: Complex dielectric constant

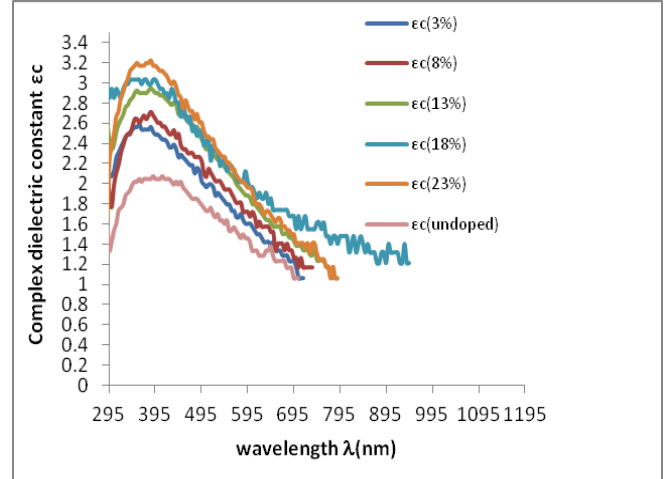


Fig. 7: Variation of Complex dielectric constant with percentage doping for MgCo₂O₄ nanofilm.

Fig. 7 shows that the complex dielectric constant of the film is maximum in the UV region and decreases to minimum in the VIS -NIR regions of electromagnetic spectrum. The complex dielectric constant increases with increasing percentage doping with cobalt.

4.8: Optical conductivity

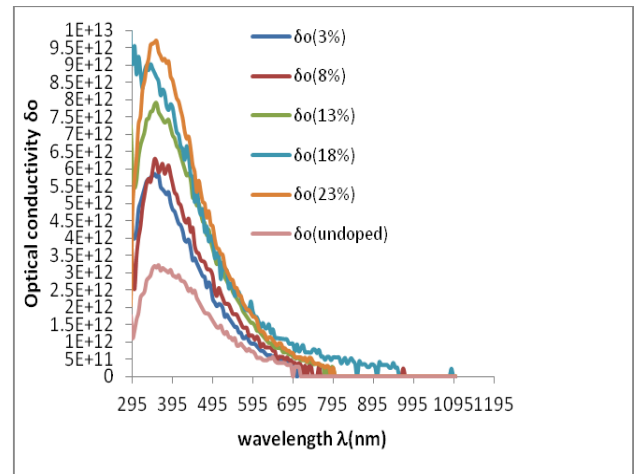


Fig. 8: Variation of Optical conductivity with percentage doping for MgCo₂O₄ nanofilm

Fig. 8 shows that the optical conductivity of the film is maximum in the UV region and decreases to zero in the NIR region of electromagnetic spectrum. The optical conductivity increases with increasing percentage doping with cobalt.

4.9: MORPHOLOGICAL ANALYSIS

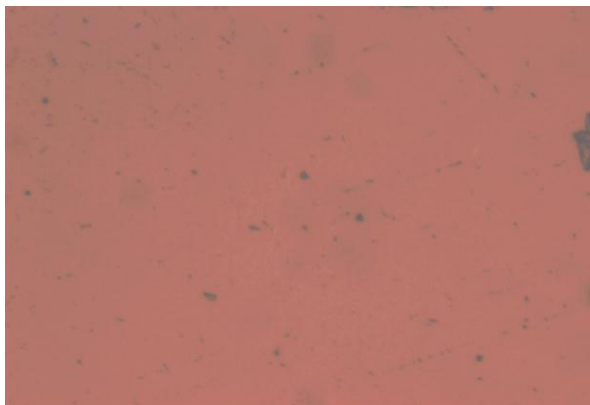


Fig. 9: Optical micrograph of MgCo₂O₄ nanofilm.

The micrograph as shown in fig. 9 reveals the film as being uniformly deposited and polycrystalline

4.10: COMPOSITIONAL ANALYSIS

Table 2: Compositional analysis for Magnesium cobalt oxide nanofilm

Sample	Percentage doping	Mg	O	Co
N23	3	58.4863	39.7022	1.8089
N14	8	55.4744	39.7018	4.8238
N24	13	52.4590	39.7023	7.8387
N25	18	49.4438	39.7026	10.8536
N26	23	46.4306	39.7009	13.8685

4.11: Structural analysis for Magnesium cobalt oxide nanofilm

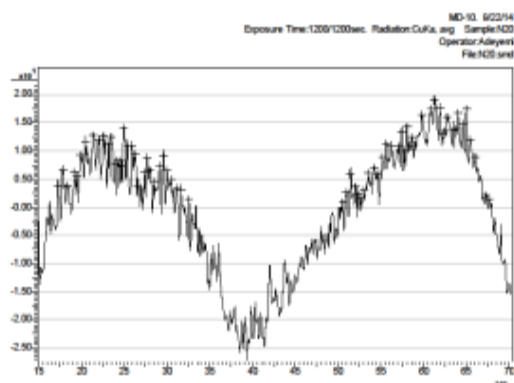


Fig. 10: XRD Pattern of MgCo₂O₄ nanofilm

5.0 : DISCUSSIONS

The films generally have low absorbance due to their ultrathin nature. From fig. 1, the absorbance is maximum in the UV region, (23% : 0.08=8%) and decreases to zero in the NIR region. Absorbance is directly proportional to the percentage doping with cobalt. As shown in fig. 2, the transmittance of the films is generally high in all the regions

(UV-VIS-NIR), with minimum in the UV region (23% doped: 84%) and increases to maximum in NIR(≈100%). This property makes the films good material for phosphors, solar cell and photothermal application. Fig. 3 shows that the reflectance of the films is generally low with maximum value of 0.0781≈7.8% for 23% doped and decreases to zero in the NIR . This property makes it a good material for antireflection coating. By virtue of its low absorbance and low reflectance in UV, VIS, NIR regions of electromagnetic spectrum, the film could be used for Photo thermal application, Photovoltaic cells and Phosphors. Reflectance is directly proportional to the percentage doping with cobalt. Result as shown in fig. 4, shows that the refractive index of the doped films is generally high in the UV region with 23% doped having maximum (1.78) while 3% doped has minimum (1.6). The undoped film has refractive index of 1.4. However, refractive index decreases to minimum in the VIS-NIR region. This makes the film a good material for antireflection film stack. The refractive index is directly proportional to the percentage doping with cobalt. From fig. 5,6,7, and 8, the films exhibit maximum extinction coefficient, electrical conductivity, complex dielectric constant, and optical conductivity respectively, in the UV region. Optical conductivity and extinction coefficient decrease to zero in the NIR while electrical conductivity and complex dielectric constant decrease to their minimum in the NIR. The optical properties viz; absorbance, reflectance, refractive index, extinction coefficient, electrical conductivity, complex dielectric constant and optical conductivity of the films are directly proportional to the percentage doping with cobalt while the transmittance is in inverse proportion. As a dilute magnetic semiconductor, MgCo₂O₄ finds good application in Spintronics, hard disks, magnetic discs, micro drive. Result of XRD analysis shows that the film has cubic structure with mean crystallite size of 1.907nm, dislocation density of 0.275lines/nm² and microstrain of 0.2160.

6.0: CONCLUSION

Cobalt doped Magnesium oxide nanofilm could be grown by electrodeposition method.

The Optical properties of the film viz; absorbance, reflectance, refractive index, extinction coefficient, electrical conductivity, complex dielectric constant, and optical conductivity are directly proportional to percentage doping with cobalt while transmittance is inversely proportional.

7.0: REFERENCES

- [1] Saraiva Marta, Sputter deposition of MgO thin film-effect of cation substitution, PhD thesis, University of Gent. 113, (2012).
- [2] Yi, X., W. Wenzhong, Q. Yitai, Y. Li and C. Zhiwen, Deposition and microstructural characterization of MgO thin films by a spray pyrolysis method, Surface Coatings Technology, 82, 291-293, (1996).
- [3] T. Ishiguro, Y. Hiroshima, T. Inoue , MgO(200) Highly Oriented Films on Si(100) Synthesized by Ambient-Controlled Pulsed KrF Excimer Laser Deposition Method ,Japanese Journal Of Applied Physics. 33(1), 3537, (1996).

- [4] I. Shih, S.L. Wu, L. Li, C.X. Qiu, P. Grant, M.W. Denhoff, Effects of heat treatment on a MgO/Si structure: a possible buffer layer structure for high- T_c superconductors, *Materials Letters.*, 11(5-7), 161-163, (1991).
- [5] J.-G. Yoon, K. Kim, Growth of (111) oriented MgO film on Si substrate by sol-gel method, *Applied Physics Letters*, 66 (20), 2661-2663, (1995).
- [6] Y. Li, G. Xiong, G. Lian, J. Li, Z. Gan, *Thin Solid Films*, 11, 223, (1993).
- [7] J.M. Zeng, H. Wang, S.X. Shang, Z. Wang, M. Wang, Preparation and characterization of epitaxial MgO thin film by atmospheric chemical vapour deposition, *Journal of Crystal Growth*, 169(3), 474-479, (1996).
- [8] Jeffrey W. Bullard, Zhengkui Xu, Mohan Menon, A novel thin film phase of oriented MgO grown from a liquid solution, *Journal of Crystal Growth*, 233, 389-398, (2001).
- [9] M. Gurvitch, A.T. Fiory, Preparation and substrate reactions of superconducting Y-Ba-Cu-O films *Applied Physics Letters*, 51, 1027, (1987).
- [10] R.B. Laibowitz, R.H. Koch, P. Chaudhari, R.J. Gambino, Thin superconducting oxide films, *Physical Review B*, 35, 8821 (1987).
- [11] T. Jüstel, H. Nikol, Optimization of luminescent materials for plasma display panels, *Advanced Materials*, 12, 527-530, (2000).
- [12] B. P. Gila, M. Hlad, A. H. Onstine, R. Frazier, G. T. Thaler, A. Herrero, E. Lambers, C. R. Abernathy, S. J. Peartona, T. Anderson, S. Jang, F. Ren, N. Moser, R. C. Fitch, and M. Freund, Improved oxide passivation of AlGaIn/GaN high electron mobility transistors, *Applied Physics Letters*, 87, 163503, 2005.
- [13] S.J. Pearton, A.G. Baca, R.D. Briggs, R.J. Shul, C. Monier, J. Han, Influence of MgO and Sc_2O_3 passivation on AlGaIn/GaN high electron mobility transistors, *Applied Physics Letters*, 80(9), 1661-1663, (2002).
- [14] D.K. Fork, F.A. Ponce, J.C. Tramontana, T.H. Geballe, Epitaxial MgO on Si(001) for Y-Ba-Cu-O thin film growth by pulsed layer deposition, *Applied Physics Letters*, 58(20), 2294-2296, (1991).
- [15] Wang L.Y., Yang J.C. Transesterification of Soybean Oil with Nano-MgO or not in Supercritical and Subcritical Methanol, *Fuel*, 86(3), 328-33, (2007).
- [16] I.V. Mishakov, V.I. Zaikovskii, D.S. Heroux, A.F. Bedilo, V.V. Chesnokov, A.M. Volodin, I.N. Martyanov, S.V. Filimonova, V.N. Parmon, K.J. Klabunde, CF_2Cl_2 Decomposition over Nanocrystalline MgO: Evidence for Long Induction Periods, *Journal of Physical Chemistry B*, 109(15), 6982-9, (2005).
- [17] G.W. Wagner, P.W. Bartram, O. Koper, K.J. Klabunde, Reactions of VX, GD and HD with nanosize MgO, *Journal of Physical Chemistry B*, 103(16), 3225-8, (1999).
- [18] S.G. Kim, J.Y. Kim, H.J. Kim, Deposition of MgO thin films by modified electrostatic spray pyrolysis method, *Thin Solid Films*, 376(1), 110-114, (2000).
- [19] P.K. Stoimenov, R.L. Klinger, G.L. Marchin, K.J. Klabunde, Metal Oxide Nanoparticles as Bactericidal Agents, *Langmuir*, 18, 6679-86, (2000).
- [20] Rubby Das and Suman Pandey, Comparison of optical properties of bulk and nano crystalline thin films of CdS using different precursors, *International journal of material science*, 1(1), 35-40, (2011).
- [21] A. Bakr Nabeel, A. M. Funde, V.S. Waman, M.M. Kambe, R.R. Hawaldar, D.P. Amalnerkar, S.W. Gosavi, and S.R. Jadkar, Determination of the optical parameters of a-Si:H thin films deposited by hot wire-chemical vapour deposition technique using transmission spectrum only, *Pramana: Journal of Physics*, 76(3), 519-531, (2011).
- [22] P. Sharma and S.C. Katyal, Determination of optical parameters of a-(As₂Se₃)₉₀Ge₁₀ thin film, *Journal of Physics D.*, 40(7), article 038, 2115-2120, (2007).
- [23] K.L. Chopra, *Thin film phenomena*, McGraw-Hill Book company, USA, 729, (1969).